

Separation of aqueous salt solution by pervaporation through hybrid organic-inorganic membrane: effect of operating conditions

Zongli Xie^{a,b}, Derrick Ng^a, Manh Hoang^a, Tuan Duong^a, Stephen Gray^b

a CSIRO Materials Science and Engineering, Private Bag 33, Clayton South, Vic.3169, Australia (Email: zongli.xie@csiro.au; manh.hoang@csiro.au; tuan.duong@csiro.au; derrick.ng@csiro.au)

b Institute for Sustainability and Innovation, Victoria University, PO Box 14428, Melbourne, Vic. 8001, Australia (E-mail: stephen.gray@vu.edu.au)

Abstract

Hybrid polymer-inorganic membranes were prepared by crosslinking poly(vinyl alcohol) (PVA), maleic acid (MA) and silica via an aqueous sol-gel route. Membrane characterisation results revealed silica nanoparticles (<10 nm) were well dispersed in the polymer matrix and significantly reduced swelling of the membrane. The membranes were tested for pervaporation separation of aqueous salt solution with NaCl concentrations of 0.2-5.0 wt% at temperatures 20-65°C, feed flowrates 30-150 mL/min and permeate pressures 2-40 Torr. The salt rejection remained high (up to 99.9%) under all operating conditions. A high water flux of 11.7 kg/m²·hr could be achieved at a feed temperature of 65°C and a vacuum of 6 Torr. The effect of operating conditions on water flux is discussed in relation to diffusion coefficients of water and fundamental transport mechanism through the membrane. The activation energy for water permeation was found to vary from 23.8 to 20.1 kJ/kmol when the salt concentration in the feed was increased from 0.2 to 5.0 wt%.

Keywords: pervaporation; hybrid organic-inorganic membranes; PVA; salt rejection

1. Introduction

Pervaporation processes are able to separate mixtures in contact with a membrane via preferentially removing one component from the mixture due to its higher affinity with, and/or faster diffusion through the membrane. In order to ensure continuous mass transport, very low absolute pressures are usually maintained on the downstream side of the membrane, removing all molecules migrating to the surface, and thus rendering a concentration difference across the membrane [1]. The mechanism of mass transfer of liquids across non-porous polymeric membranes includes successive stages of sorption of a liquid and its diffusion through the free volume of the polymeric material [2].

Pervaporation has been extensively used for separation or concentration of mixtures of aqueous-organic or organic liquids. However, there are only limited studies on application of this technology for water desalination [2, 3]. In desalination applications, pervaporation has the advantage of near 100% of salt rejection and potential low energy consumption. The pervaporation of an aqueous salt solution can be regarded as separation of a pseudo-liquid mixture containing free water molecules and bulkier hydrated ions formed in solution upon dissociation of the salt in water [2]. A summary of previously reported open literature on desalination by pervaporation is presented in Table 1 [4]. The water flux in systems reported so far is generally low, at $<6 \text{ kg/m}^2\cdot\text{hr}$. The feed temperature was found to be a crucial parameter due to the increase in diffusivity and reduction in viscosity that occurs on heating. In addition, the vacuum, the membrane thickness and the inherent permeability of the membrane polymer are also important.

Table 1: summary of previous studies on pervaporation desalination (adapted from ref. [4]).

Membrane Polymer	Feed Conc., g/L	Temp., °C	Membrane Thickness, μm	Flux, $\text{kg/m}^2\text{h}$	Reference
Cotton cellulose	40	40	30	6.1	[2]
Cellulose diacetate on MD membrane	40	40	0.5-1.5	4.1-5.1	
Sulphonated PE, cation exchanger	0-176	25-65	100	0.8-3.3	[5]
Quaternised PE, anion exchanger	0-176	45-65	50-180	1.5-3.0	[6]
	35	60	70	2.3	
	35	60	170	0.5	
Polyether amide	35	Solar, 46-82	40	0.2	[3]
Polyether ester	3.2-5.2	Solar,	160	0.15	[7]
	9.9-18	22-29		0.13	
	20-30			0.12	

Poly(vinyl alcohol) (PVA) membranes have been studied extensively as pervaporation materials in various applications due to its excellent film-forming and highly hydrophilic properties. PVA membranes are known to exhibit high degrees of swelling in aqueous solutions due to the presence of hydroxyl groups [8-10]. To improve the performance and stability of PVA membranes in the aqueous solution, it is necessary to insolubilise or modify the membrane by crosslinking or addition of hydrophobic groups to achieve a stable membrane with good mechanical properties and selective permeability to water. Incorporation of inorganic particles in PVA membranes to form hybrid organic-inorganic membranes has been one such technique to improve the stability and separation performance of PVA membranes [11, 12].

In our recent work, the pervaporation separation of aqueous salt solution was carried out to evaluate the pervaporation performance of hybrid organic-inorganic membranes based on PVA, maleic acid (MA) and silica [13]. We found that the hybrid PVA/MA/silica membrane showed superior performance with a high water flux (up to 5.5 kg/m².hr) and a very high salt rejection (up to 99.9%). Chemical crosslinking among PVA, MA and silica inhibited the swelling of PVA and led to a compact and stable structure. The introduction of silica nanoparticles in the polymer matrix enhanced both the water flux and salt rejection due to increased diffusion coefficients of water through the membrane.

It is well known that the pervaporation performance is not only dependent on the properties of membranes, but also the operation conditions such as feed concentration, temperature, permeate pressure and feed flowrate [14]. For scale up, it is important to design and operate the system under optimum operating conditions to make the process more efficient and also economically viable. The objective of this work is to study the effect of operating conditions on pervaporation separation performance of aqueous salt solutions. A synthesised hybrid PVA/MA/silica membrane was tested for separation of aqueous salt solution by the pervaporation process at various salt concentrations and operating conditions. The activation energy of permeation was calculated from the Arrhenius relationship. The performance was discussed in relation to the diffusion coefficient of water to understand the fundamental transport mechanism within the membrane.

2. Experimental

2.1 Hybrid membrane synthesis and characterisation

The hybrid PVA/MA/silica membrane containing 5 wt% MA and 10 wt% SiO₂ with respect to PVA was synthesised via an aqueous sol-gel route. Reagent grade chemicals including PVA (98-99% hydrolysed, average MW 160,000), tetraethyl orthosilicate (TEOS, 98%), maleic acid (MA), *p*-toluene sulfonic acid (98.5%, monohydrate) were obtained from Sigma-Aldrich and used without further purification.

PVA polymer powder (8.0g) was first dissolved in 100 mL Milli-Q deionised water (18.1 MΩ·cm at 25°C) at 95°C. The obtained 8 wt% PVA solution was left to cool to room temperature, followed by addition 0.4g of MA and 0.08 g of *p*-toluene sulfonic acid into the solution (pH 1.9±0.1). A premixed 2.78g TEOS and 25.0g ethanol

mixture (weight ratio of TEOS:ethanol =1:9) was added drop wise to the above PVA solution under steady stirring and continuously stirred for another 2 hours. The resulting homogeneous mixture was cast on Perspex Petri dishes to the desired thickness and dried in air followed by heat treatment in a fan forced oven at 140°C for 2 hours. A pure PVA membrane sample was also prepared as a reference for comparison. The thickness of membranes was measured at different points across the membrane using a Fowler electronic digital micrometer (accuracy $\pm 1 \mu\text{m}$) and the membranes used in this study had an average thickness of 20 μm .

Energy dispersive X-ray spectrometry (EDS) of the hybrid membrane was performed by an EDAX detector on a Philips XL30 scanning electronic microscope (SEM) with a voltage of 15 kV and a working distance of 15 mm. Samples were coated by sputtering with carbon. The morphology of the hybrid membrane sample was imaged using a TECNAI F30 Transmission electron microscope (TEM) with an accelerating voltage of 200 kV. TEM samples were prepared by a focused ion beam (FIB) technique. The hydrophilic properties of membrane samples were assessed by a KSV contact angle meter (CAM200) equipped with a video capturing system. Static contact angles were measured by the sessile drop method. A 6 μL water drop was formed on the levelled surface of the membrane for contact angle measurements.

The water uptake of PVA and PVA/MA/silica hybrid membrane was measured by the following procedures: (1) Immersing the dried membrane in deionised water at room temperature for 48 h to reach the absorption equilibrium. (2) Blotting surface of wet membrane with the cleansing tissue to remove surface water and quickly weighing the wet membrane within 10 sec (W_s). (3) Drying the membrane in a vacuum oven at 50°C for overnight and then weighing again to obtain the mass of dried membrane (W_d). The water uptake of membrane was then calculated according to:

$$\text{Water uptake} = (W_s - W_d)/W_d \times 100\% \quad (1)$$

2.2 Pervaporation testing

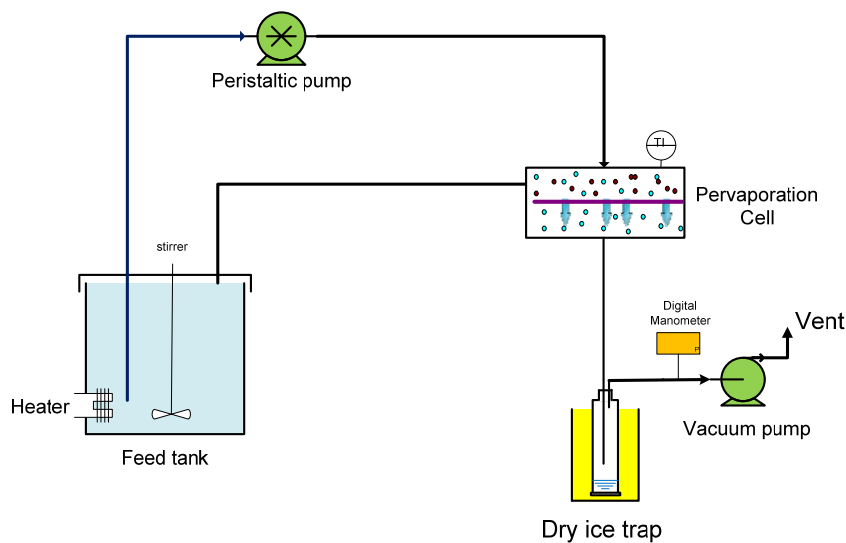


Figure 1. Schematic drawing of the pervaporation unit.

The pervaporation experiments were carried out on a laboratory scale pervaporation unit as shown in Figure 1. The membrane was placed in the middle of a pervaporation cell with an effective surface area of the membrane of 12.6 cm². During the experiment, the feed solution was preheated in a water bath to a desired temperature and pumped to the pervaporation cell using a Masterflex[®] peristaltic pump. The pressure on the permeate side of the membrane cell was maintained at constant pressure with a vacuum pump. The permeate was collected in a dry-ice cold trap. A K-type thermocouple installed in the feed chamber was used to measure the operating temperature of feed solution and the feed temperature was varied from 22 to 65°C in this study.

An aqueous salt solution containing 0.2-5.0wt% NaCl was used as the feed solution. The range of salt concentration in the feed solution was chosen to represent the typical salt level of brackish water, sea water and brine stream, respectively.

The pervaporation separation performance of aqueous salt solution of hybrid membranes were characterised by water flux and salt rejection. The water flux (J) was determined from the mass (M) of permeate collected in the cold trap, the effective membrane area (A) and the experimental time (t).

$$J = M / At \quad (2)$$

The salt concentration of the feed and permeate were derived from measured conductivity with an Oakton[®] Con 110 conductivity meter. The salt rejection (R) was determined by the following equation:

$$R = (C_f - C_p) / C_f \quad (3)$$

where C_f and C_p are NaCl concentration in the feed and permeate, respectively.

The apparent diffusion coefficient of water was calculated from a simplified equation derived from Fick's law [15]:

$$D = \frac{J\delta}{C_f} \quad (4)$$

Where δ is the membrane thickness, and C_f is the concentration of water at the membrane feed side.

3. Results

3.1 Membrane characterisation

In the hybrid PVA/MA/silica membrane, it is believed that silica nanoparticles, which result from the hydrolysis and condensation of TEOS in casting solution, change the

nanostructure of the hybrid membrane and consequently lead to the improved physical properties and performance [11, 12]. Figure 2 shows the morphology of the hybrid PVA/MA/silica membrane. The TEM image indicates the silica is highly dispersed within the polymer matrix, no particles or agglomerations greater than 10 nm being observed (Fig.2). The SEM-EDS was performed at various locations across the hybrid membrane and the typical EDS spectra are shown in Figure 3. EDS spectra further confirmed the formation of silica particles and their uniform distribution throughout the membrane.

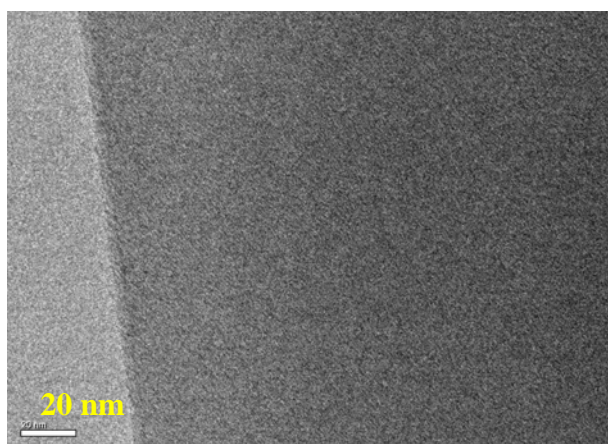


Figure 2: TEM image of hybrid PVA/MA/silica membrane (containing 5 wt% MA and 10 wt% SiO₂ with respect to PVA).

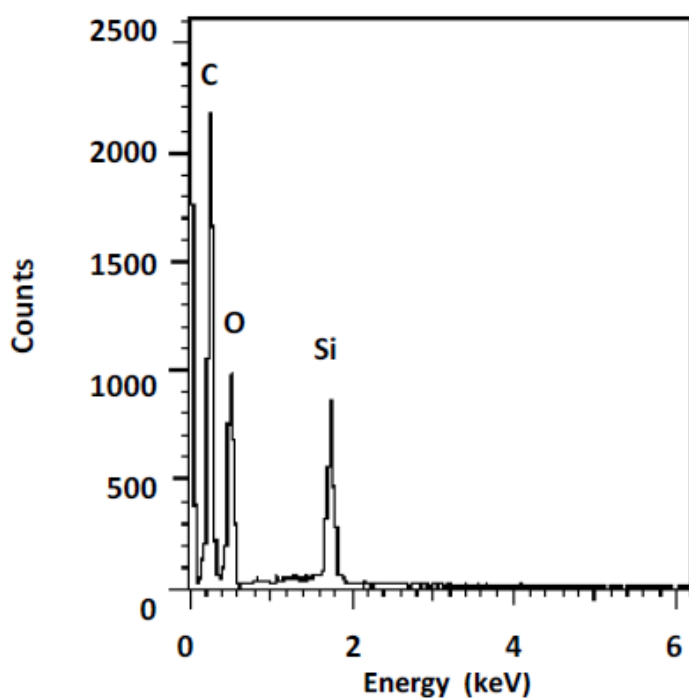


Figure 3. EDS spectra of hybrid PVA/MA/silica membrane (containing 5 wt% MA and 10 wt% SiO₂ with respect to PVA).

Table 2 shows the contact angle and water uptake of hybrid PVA/MA/silica membrane. The results on a pure PVA membrane are also shown for comparison. As can be seen, the water uptake of the hybrid membrane has been greatly reduced, indicating suppressed swelling due to crosslinking among PVA, MA and silica. The hybrid membrane remained hydrophilic. This could be due to the contribution of hydrophilic–OH groups from silanol that resulted from hydrolysis and condensation reactions of TEOS. The high hydrophilicity and reasonable equilibrium swelling indicated the potential for higher water permeability of the membrane.

Table 2: Contact angle and water uptake of PVA and PVA/MA/silica membrane

	PVA, 5%MA, 10%silica	PVA
Contact angle (± 2 degree)	51.5	43.0
Water uptake (%)	$36 \pm 5\%$	$480 \pm 30\%$

3.2 Salt rejection

In this study, the salt (NaCl) rejection remained high (about 99.9%) irrespective of variation in operating conditions. This is not surprising. Firstly, NaCl is a non-volatile compound and it is unlikely to enter the vapour stream on the permeate side. This low volatility of NaCl will lead to high salt rejection in the pervaporation process. Varying operating conditions could have significant effect on the transmembrane concentration (driving force for mass transport of the pervaporation membrane) of water but not on salt. Therefore, the operating condition has no effect on the salt rejection. Secondly, according to the solution-diffusion model, the sorption selectivity is more dependent on the affinity between the PVA and the permeants in the solution step. As the hybrid PVA/MA/silica membrane used in the study is hydrophilic in nature (Table 2) and the major component in the feed solution is water, the water molecules will be preferentially diffused and permeated into the membrane [12]. As a result, the salt rejection remained high. Thirdly, in our recent work, we have found, for hybrid PVA/MA/silica membranes, the crosslinking among PVA, MA and silica resulted in a more rigid, compact structure. In particular, the incorporation of silica nanoparticles in the polymer chain may disrupt the polymer chain packing and therefore leading to a high salt rejection. In the following section, only effects of operating conditions on water flux are discussed.

3.3 Effect of feed concentration

Figure 4 shows the effect of salt concentration in the feed solution on separation performance of aqueous salt solution at various feed temperatures. At room temperature, salt concentration has negligible effect on water flux. At a higher temperatures (50°C), the water flux decreases with increasing salt concentration. This increase became more significant as the feed temperature was increased further to 65°C.

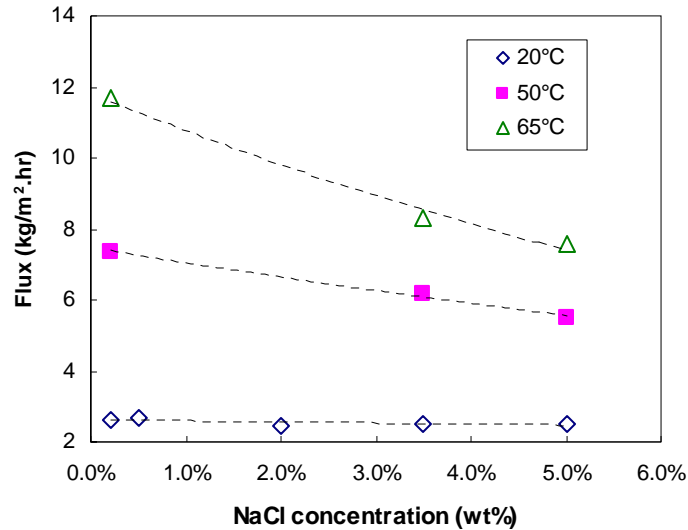


Figure 4. Effect of feed concentration on water flux (membrane thickness 20 μm , feed flowrate 30 mL/min, vacuum 6 Torr)

Feed concentration is believed to directly affect the sorption of its components at the liquid/membrane interface [14]. That is, the concentration of the components in the membrane tends to increase with its increase in the feed concentration. Since diffusion in the membrane is concentration dependant, the permeate flux generally increases with the bulk feed concentration. As the salt concentration increased from 0.2 wt% to 5.0 wt%, the water concentration decreased from 99.8 wt% to 95.0 wt%. At room temperature, this decrease in water concentration may not have any effect on diffusion within the membrane as the majority of the feed is water and there is no major difference of water vapour pressure at salt concentration range of 95.0-99.8%. It is therefore expected that the diffusivity of the membrane towards water remained constant at room temperature. Therefore, there was no or negligible change on the flux. On the other hand, at the higher temperatures, as the vapour pressure is exponentially related to the temperature, differences in bulk feed water concentration would have pronounced effect on the water concentration in the membrane surface, and consequently affect the diffusivity and flux. Therefore, it is expected that, at the higher temperature, that increasing salt concentration would lead to a decrease in diffusivity in the membrane due to the decreased water concentration. The trend in variation of diffusion coefficients of water has been confirmed by the calculated apparent diffusivity results as shown in Table 3.

Table 3: Apparent diffusion coefficients of water at various salt concentrations and feed temperatures.

Salt concentration	Diffusion coefficient of water ($10^{-11} \text{ m}^2/\text{s}$)		
	20°C	50°C	65°C
0.2 wt%	1.45	4.09	6.51
3.0 wt%	1.45	3.56	4.78
5.0 wt%	1.47	3.22	4.42

3.4 Effect of feed flow rate

Figure 5 shows the effect of the feed flowrate on the pervaporation performance of the hybrid PVA/MA/silica membrane when the feed flowrate varied from 30-110 mL/min at a feed temperature of 22°C. It seems the feed flowrate has little or negligible effect on the water flux. The water flux remained constant at around 2.5 kg/m²·hr over the feed flowrate range of 30-150 mL/min.

Mass transfer in the liquid feed side may be limited by the extent of concentration polarisation. Generally an increase of feed flowrate reduces concentration polarisation and increases flux due to a reduction of transport resistance in liquid boundary layer [14]. However, this positive effect is not observed in the study. In the studied feed flowrate range, the feed velocity varied from 0.4-1.99 x 10⁻³ m/s. The corresponding Reynolds numbers are 21-105, indicating that the flow is in the laminar flow regime. This implies that increasing feed flowrate had little effect on the turbulence and fluid dynamics of the feed stream in the laminar flow region, and the mass transfer from the feed to the membrane was not a rate limiting step. Therefore, concentration polarisation is not a significant issue for these experiments.

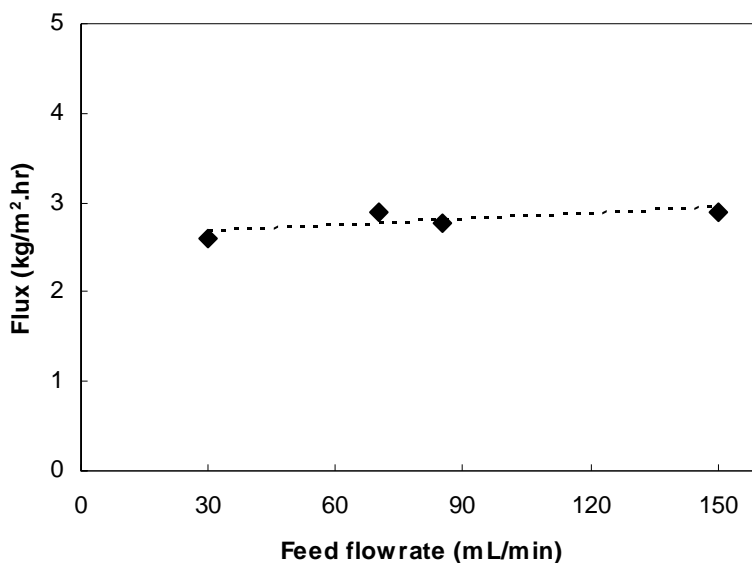


Figure 5. Effect of feed flowrate on water flux (membrane thickness 20 μm, feed temperature 22°C, vacuum 6 Torr)

Table 4 presents the diffusion coefficient of water at various feed flowrate. The diffusion coefficient remained almost constant over the studied flowrate range, again confirming that the rate of pervaporation was not affected by the feed flowrate and therefore the transport of water to the membrane surface.

Table 4: Apparent diffusion coefficients of water at various feed flowrate (feed temperature 22°C, vacuum 6 Torr).

Feed flowrate (mL/min)	30	70	85	150
Feed velocity (10^{-3} m/s)	0.40	0.93	1.13	1.99
Diffusion coefficient of water (10^{-11} m ² /s)	1.46	1.60	1.54	1.61

3.5 Effect of permeate pressure

Permeate pressure is another important operating parameter as a high vacuum is directly related to a high energy cost. Theoretically, the maximum flux is achieved at zero absolute permeate pressure. Figure 6 shows the effect of permeate pressure on water flux. Generally, the water flux decreased as the permeate pressure is increased since there is a decrease of driving force for mass transport. For pervaporation processes, the driving force is provided by the vapour pressure difference between the feed and permeate side of the membrane. With increasing permeate pressure (i.e. decreasing vacuum), as the feed side pressure remains unchanged, the transmembrane vapour pressure difference is increased. This leads to a decreased driving force and consequently water flux.

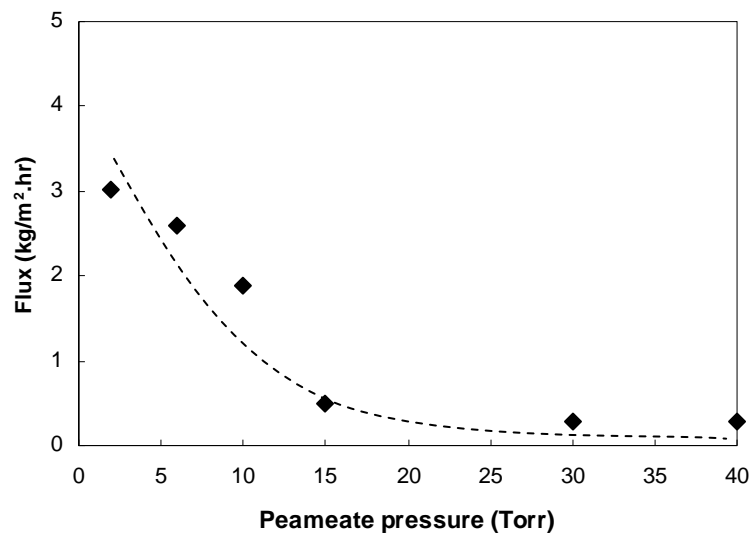


Figure 6. Effect of vacuum on water flux (membrane thickness 20 μ m, feed temperature 20°C, feed flowrate 30 mL/min)

It was observed that the water flux dropped down to less than 0.5 kg/m²·hr when the permeate pressure increased to >15 Torr. At room temperature, the saturation vapour pressure of water is about 17 Torr [16]. When the permeate pressure is increased above 15 Torr, the driving force for water vaporisation approaches zero, leading to near zero net evaporation and consequently the low mass transport of water. Table 5 presents the diffusion coefficient of water at various permeate pressure. Decreasing diffusion coefficient with permeate pressure indicates that the permeation process is mainly controlled by diffusion through the hybrid membrane. As permeate pressure

increased above 15 Torr, the diffusion coefficient dropped significantly, by nearly 90%, indicating the diffusion of water has been greatly reduced.

Table 5: Apparent diffusion coefficients of water at various permeate pressure (feed temperature 20°C, feed flowrate 30 mL/min).

Permeate pressure (Torr)	2	6	10	15	30	40
Diffusion coefficient (10^{-11} m ² /s)	1.68	1.45	1.05	0.28	0.16	0.16

3.6 Effect of feed temperature

Figure 7 shows the effect of feed temperature on the pervaporation desalination performance of hybrid PVA/MA/silica membrane at a feed flowrate of 30 mL/min and a vacuum 6 Torr. For all feed concentrations, there was an exponential increase of water flux when the feed temperature increased from 20°C to 65°C. A high water flux of 11.7 kg/m²·hr was achieved at the feed temperature of 65°C. This is not surprising, as firstly, the driving force for the pervaporation process is the partial vapour pressure difference of permeant between the feed and permeate conditions. As the feed temperature increased, the water vapour pressure on the feed side increased exponentially. As the vapour pressure on the permeate side was held constant, the increasing vapour pressure in feed led to an increase in the driving force and consequently the water flux. Secondly, an increase in temperature also raises the diffusion coefficient for transport through the membrane, making it easier for the transport of the water molecules. This is confirmed by the diffusion coefficient results as shown in Table 2. As can be seen, there is an increasing trend in the diffusivity coefficient of water in the hybrid membrane as the feed temperature rose. In addition, the mobility of the polymer chains also increased with the feed temperature, which led to the increase of the free volume of the membranes. According to the free volume theory [17], the thermal motion of polymer chains in the amorphous region creates momentary free volumes. As the temperature increases, the frequency and amplitude of the chain motion increase and the resulting free volumes become larger. Consequently, water molecules which have smaller size can diffuse through these free volumes more easily. Therefore, the water flux increases.

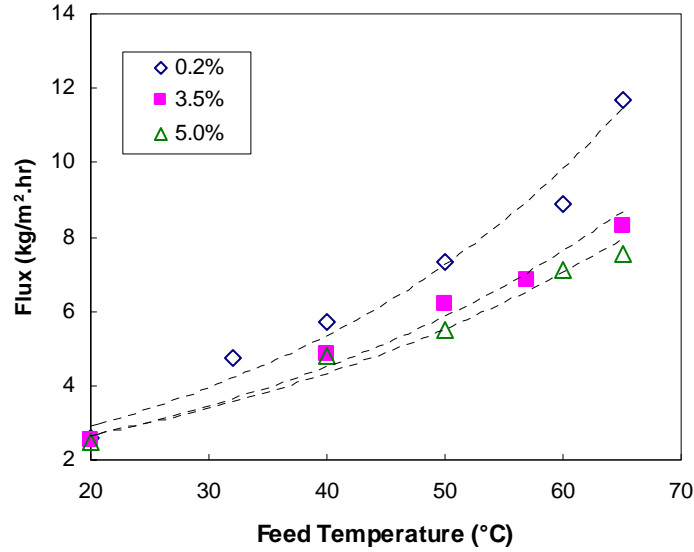


Figure 7. Effect of feed temperature on water flux (membrane thickness 20 μm , feed flowrate 30 mL/min, vacuum 6 Torr)

The temperature dependence of permeate flux for pervaporation generally follows an Arrhenius type relationship [10, 11, 14].

$$J_i = A_i \exp\left(-\frac{E_{p,i}}{RT}\right) \quad (5)$$

Where J_i is the permeate flux of i , A_i is the pre-exponential factor, R is the gas constant, T is the absolute temperature and $E_{p,i}$ is the apparent activation energy for permeation which depends on both the activation energy for diffusion and heat of sorption.

Figure 8 shows the Arrhenius plot of the water flux and feed temperature at different feed concentrations. The linear relationship was observed between fluxes and the reciprocal of the absolute temperature. The activation energy of permeation of water ($E_{p,w}$) in the membrane was taken from the slope of the Arrhenius plot (equation 1) and the results are shown in Table 6. There was no significant variation in activation energy of permeation of water as the salt concentration in the feed solution increased from 0.2 to 5.0wt%, with the activation energy varying from 23.8 to 20.1 kJ/kmol. The positive activation energy implies that permeation flux increases with increasing temperature [8], as confirmed from the results shown in Figure 7. The relatively low activation energy could be attributed to the high water content over the studied feed concentration range. At the higher water content in the feed, the significance of the plasticising effect of water on the membrane can significantly enhance free volume and diffusion of water. Therefore, the activation energy is low. As explained by Jiratananon *et al.* [14], an increase of temperature can reduce the amount of water-water clusters. As a result, the permeation of water is significantly enhanced.

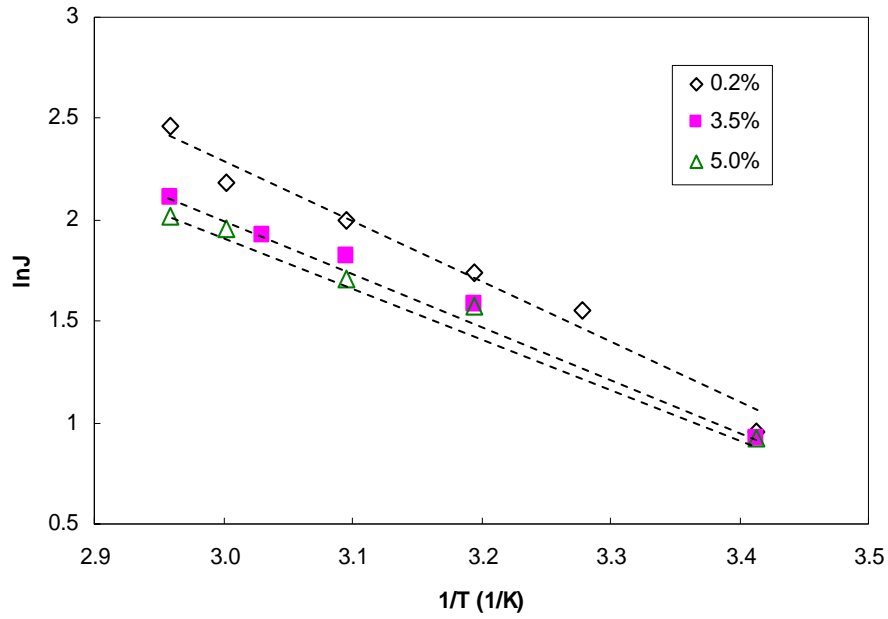


Figure 8. Arrhenius plot of the water flux at various feed concentrations.

Table 6: Activation energy of permeation of water at different feed concentration (feed flowrate 30 mL/min, vacuum 6 Torr).

NaCl concentration	0.2 wt%	3.0 wt%	5.0 wt%
Activation energy (kJ/kmol)	23.8	21.6	20.1

4. Conclusions

Pervaporation under various operating conditions was carried out to evaluate the separation performance of aqueous salt solution through the hybrid PVA/MA/silica membrane. A high water flux of $11.7 \text{ kg/m}^2\cdot\text{hr}$ could be achieved at a feed temperature of 65°C and a vacuum of 6 Torr. Under all operating conditions, salt rejection remain high (up to 99.9%), indicating salt rejection performance of hybrid PVA/MA/silica membrane is independent of the operating conditions due to the non-volatile nature of NaCl. In the studied laminar flow region, feed flowrate had little or negligible effect on the water flux and diffusion coefficients of water, and this confirmed that the sorption of water onto the membrane surface was not the rate controlling step of pervaporation separation of aqueous salt solution. High feed temperature and high vacuum had a significant enhancing effect on the water flux and diffusivity coefficients of water due to the increased driving force and increased free volume of the membrane. The activation energy of permeation of water was found to vary from 23.8 to 20.1 kJ/kmol when the salt concentration in the feed was increased from 0.2 to 5.0 wt%. The effect of feed concentration had differing impacts depending on the operating temperature. At low feed temperatures, the salt concentration in the feed solution had little or negligible effect on water flux and diffusion coefficients. However, at high feed temperature ($50\text{-}60^\circ\text{C}$), feed flux and diffusivity of water decreased with increasing salt concentration due to the decreased water vapour pressure and consequently water concentration in the membrane surface.

Acknowledgement

The authors would like to acknowledge the CSIRO Water for Healthy Country National Research Flagship for the financial support of this work. Dr Mary She and Juan Zhang from Deakin University are greatly acknowledged for their kind help in TEM work. Buu Dao from CSIRO is also acknowledged for the helpful discussion.

References

- [1] P. Shao and R. Y. M. Huang, *Journal of Membrane Science* **287** (2007), pp 162.
- [2] Y. P. Kuznetsov, E. V. Kruchinina, Y. G. Baklagina, A. K. Khripunov and O. A. Tulupova, *Russian Journal of Applied Chemistry* **80** (2007), pp 790.
- [3] H. J. Zwijnenberg, G. H. Koops and M. Wessling, *Journal of Membrane Science* **250** (2005), pp 235.
- [4] B. Bolto, M. Hoang and Z. Xie, *Water AWA* **37** (2010), pp 77.
- [5] E. Korin, I. Ladizhensky and E. Korngold, *Chemical Engineering and Processing* **35** (1996), pp 451.
- [6] E. Korngold, E. Korin and I. Ladizhensky, *Desalination* **107** (1996), pp 121.
- [7] E. Quiñones-Bolaños, H. Zhou, R. Soundararajan and L. Otten, *Journal of Membrane Science* **252** (2005), pp 19.
- [8] A. A. Kittur, M. Y. Kariduraganavar, U. S. Toti, K. Ramesh and T. M. Aminabhavi, *Journal of Applied Polymer Science* **90** (2003), pp 2441.
- [9] B. Bolto, T. Tran, M. Hoang and Z. Xie, *Progress in Polymer Science* **34** (2009), pp 969.
- [10] C.-K. Yeom and K.-H. Lee, *Journal of Membrane Science* **109** (1996), pp 257.
- [11] F. Peng, L. Lu, H. Sun and Z. Jiang, *Journal of Membrane Science* **281** (2006), pp 600.
- [12] T. Uragami, K. Okazaki, H. Matsugi and T. Miyata, *Macromolecules* **35** (2002), pp 9156.
- [13] Z. Xie, M. Hoang, D. Ng, T. Duong, B. Dao and S. Gray., *proceeding of IMISTEC10/AMS6 conference, 22-26 November 2010, Sydney, Australia* (2010).
- [14] R. Jiraratananon, A. Chanachai, R. Y. M. Huang and D. Uttapap, *Journal of Membrane Science* **195** (2002), pp 143.
- [15] J. P. G. Villaluenga, P. Godino, M. Khayet, B. Seoane and J. I. Mengual, *Industrial & Engineering Chemistry Research* **43** (2004), pp 2548.
- [16] B. Z. Shakhshiri, *Chemical Demonstrations: A handbook for Teachers in Chemistry*. (2nd edition), Madison: The University of Wisconsin Press, (1992).
- [17] M. C. Burshe, S. B. Sawant, J. B. Joshi and V. G. Pangarkar, *Separation and Purification Technology* **12** (1997), pp 145.